DOI: 10.24996/ijs.2025.66.4.17

Iraqi Journal of Science

ISSN: 0067-2904

Effect of Kaolin Grain Size on Its Efficiency as Anti-Seepage in the Petroleum Industry

Mayssaa. Ali Al-Bidry *, Ramzy. S. Hamied
Oil and Gas Engineering Department, University of Technology, Baghdad - Iraq

Received: 29/9/2023 Accepted: 28/4/2024 Published: 30/4/2025

Abstract

The study goals encompassed the evaluation of the effectiveness of kaolin liners in preventing the seepage of crude oil with different viscosities. The research used light and heavy crude oils sourced from Al-Barjisiah and Al-Ahdab oil fields in Iraq with kaolin grains of varying sizes. In the first stage, kaolin was analyzed using X-ray diffraction and X-ray fluorescence to identify minerals and chemical composition. The physical characteristics of crude oil were also examined. Ten liners were prepared for the test depending on kaolin grain size ranging from 300, 150, 75, 50 µm and nano size with chosen crude oil. The findings indicated that kaolin liners of various sizes could not retain light crude oil. The flow of heavy crude oil was observed to be impeded, and seepage was effectively stopped for different durations when kaolin liners of varying sizes, precisely 50 µm, 75 µm, 150 µm, and 300 µm, were employed. These durations were measured to be 54, 96, 90, and 72 hours, respectively. Partial replacement of kaolin 150 µm by nano-size kaolin improved liner ability to impede the flow of light and heavy crude oil with a long period of retention time and without seepage.

Keywords: anti-seepage crude oil, compacted clay, kaolin, liner, Nano kaolin

تأثير الحجم الحبيبي للكاؤولين على فعاليته كمضاد للتسرب في الصناعة النفطية

ميساء علي البدري* , رمزي صيهود حميد

قسم هندسة النفط والغاز ، الجامعة التكنولوجية، بغداد، العراق

الخلاصة

هدفت الدراسة إلى تقييم مدى فعالية بطانات الكاؤولين في منع تسرب النفط الخام باختلاف اللزوجة. استخدم في البحث الزيوت الخام الخفيفة والثقيلة المستخرجة من حقلي البرجسية والأحدب النفطيين في العراق مع حبيبات الكاؤولين بأحجام مختلفة. في المرحلة الأولى، تم تحليل الكاؤولين باستخدام حيود الأشعة السينية واشعة فلورسانس السينية للتعرف على المعادن والتركيب الكيميائي. كما تم فحص الخصائص الفيزيائية للنفط الخام. تم تحضير عشرة بطانات للاختبار اعتمادا على حجم حبيبات الكاؤولين تتراوح بين 300، 150، 75، 50 ميكرومتر وحجم النانو مع الزيت الخام. أشارت النتائج إلى أن بطانات الكاؤولين بمختلف أحجامها فشلت في الاحتفاظ ومنع تسرب النفط الخام الخفيف. في حين لوحظ إعاقة تدفق النفط الخام الثقيل ومنع التسرب بشكل فعال لفترات مختلفة عند استخدام بطانات الكاؤولين ذات الأحجام المختلفة، وتحديدًا 50 و75 و150 و300 ميكرومتر. ولفترات زمنية تتراوح 54، 96، 90، و72 ساعة، على التوالي. أدى الاستبدال الجزئي

*Email: mayssaa.a.abdwon@uotechnology.edu.iq

للكاؤولين 150 ميكرومتر بكاؤولين بحجم النانو إلى تحسين قدرة البطانة على إعاقة تدفق النفط الخام الخفيف والثقيل مع فترة احتجاز طويلة ودون تسرب.

1. Introduction

Kaolin, often known as China clay, is a type of mineral that mainly contains the crystal compound kaolinite ($Al_2O_3.2SiO_2.2H_2O$). The properties that set kaolin apart from other clay minerals include its whiteness, softness, and ability to dissolve easily in solutions.[1] [2]. The physical properties of kaolin make it a popular material used in ceramics, paint, polymers, and pharmaceutics [3] [4] [5]. Kaolin can remove nonpolar hydrocarbon from an aqueous environment; hence, it can be used to tackle a variety of environmental issues, including removing oil spills from the water surface [6]. The size of the kaolinite particles and their structural perfection determine the technological qualities of kaolin [7]. There is no consensus on the impact of kaolinite microcrystal size and structural perfection on technical properties. Repeated attempts to find their relation yielded no significant results. The leading cause of microcrystal structural disorder is an imperfection in the superposition of kaolinite packets on top of each other. Dislocations caused by the distortion of the kaolinite packets have a significant influence on crystal imperfection [8]. Nanoparticles are essential in various industrial applications because of their distinctive and frequently advantageous characteristics. The high surface-to-volume ratio and size effects of nanoparticles introduce several size-dependent phenomena, such as electronic, magnetic, mechanical, and chemical properties (quantum effects) [9]. Nanotechnology can be a long-term approach to improving oil spill technology because nano-sized materials can be used for specific purposes. The application of nanotechnology to oil spill recovery is a relatively new field. Several factors, including the rate of removal, sorption, and oil retention, can determine the effectiveness of a sorbent.. Sorbents have low crude oil retention and are nonselective, absorbing both oil and water. Advanced nanomaterials are attempting to address this shortcoming by improving very selective materials in oil uptake. Because nanoparticles have a higher surface area to volume ratio, they have better oil retention and sorption capacity [10] [11]. Geosynthetics have been safeguarding the environment for decades by effectively confining gasses and liquids. Geosynthetics can be used as a standalone liner or as a part of a composite liner [12]. Using bentonite liners to prevent seepage has been studied extensively [13][14] [15] [16]. Bentonite clay is commonly utilized as a pollution liner due to its low fluid permeability [13]. The effectiveness of bentonite clay as a linear agent to prevent seepage differs depending on the type of bentonite. When it comes to reducing crude oil leaks, Na-bentonite is superior to Ca-bentonite, and its effectiveness is enhanced as the grain size decreases, as mentioned Al-Bidry et al. (2017) [17]. Attapulgite has been proposed as an alternative to bentonite in compacted clay liner applications [18][19]. Attapulgite liners with varied grain sizes efficiently retain and prevent crude oil seepage, according to research by Al-Bidry and Hamied, (2022). These liners act as a primary layer to block heavy flow, but do not affect light crude oil seepage [13]. Kaolin clay is preferred in composite liner. Oyeleke et al., (2011) demonstrated that designed composite earthen sanitary landfill liners made of kaolin clay and palm oil fuel ash are appropriate for solid waste [20]. Compacted liner materials made of natural clay with kaolinite, sepiolite, and zeolite were studied by Yucel et al. (2014). They found that soil strength and metal adsorption capacities were improved with increasing sepiolite content [21]. Although compacted kaolin liners have been used as landfill liners, hazardous waste containment systems, and mining waste disposal facilities, they have received little attention as anti-seepage crude oil liners.

The current study looks into the ability of Iraqi kaolin to absorb crude oil, its potential use as an anti-crude oil seepage material, and the effect of particle sizes ranging from 300, 150, 75, 53 µm and nano grain size on the effectiveness of Iraqi kaolin as a compacted liner for crude oil leakage prevention.

2. Experimental Work

2.1 Sample preparation

Raw kaolin samples were acquired from the Iraqi Geological Survey Company. Kaolin samples were crushed into powder and mixed thoroughly to obtain a homogeneous representative sample. The crushed clay was dried under 110^o C for 10 hrs, then grinded and sieved into different grain sizes; 300, 150, 75, 50 µm and nano size. Kaolin of 50 µm was used to prepare the nano-size samples. The nano kaolin was produced in a ceramic ball mill over a seven-day grinding period [22]. X-ray diffraction (type 6100/7000 X-ray diffraction) was used for raw and nano kaolin samples to characterize the mineral composition of kaolin. To investigate chemical composition, an XRF analysis was performed using an X-ray fluorescence spectrometer. To show nano particle size distribution, a Brookhaven Instruments Crop. 90Plus particle size software Ver. 5.34 was used. Fourier transform infrared (FTIR) was carried out with a Perkin–Elmer apparatus for raw and oil-saturated kaolin samples.

2.2 Crude Oil Properties

The American Petroleum Institute (API) classifies crude oil based on its relative density. Crude oil from Iraqi oil fields was utilized to assess the behaviour of crude oil with kaolin liners: light crude oil from the Al-Burjsiha field (BF) and heavy crude oil from the Al-Ahdab field (AF). Table 1 illustrates the physical characteristics of Al-Burjsiha and Al-Ahdab crude oil examined in the basic crude oil laboratory at the Oil and Gas Engineering Department-University of Technology.

Table 1: Physical characteristics of Al-Ahdab and Al-Burjsiha crude oil.

Physical Characteristics	Al-Ahdab Oil Field	Al-Burjsiha Oil Field
API	19.82	29.71
Viscosity	3.58 CP at (100 RPM) (17.3^o C)	0.05 CP at (100 RPM) (17.3^o C)
Density	958 kg/m3	8777 kg/m3
Sulfur content %	0.64 %	0.38 %
Specific gravity	0.958	0.8777
Sediment content%	3%	1.41%

2.3 Experimental setup and procedure

Kaolin was weighed at around 100 g for the hydrocarbon retention capacity test before being placed in open-ended tubes. The test tube was mounted on a stand, and a beaker was placed beneath it to collect any free crude oil. The ground beneath the tank and pipe was then represented by the stainless steel mesh, which was then positioned at the bottom open end. A 2 kg free weight was applied on the top of the clay in a test tube for 20 min to achieve the required compaction. After that, the chosen hydrocarbon 200 mL was poured over the selected clay. For each liner, record the amount of oil draining over time and determine the kaolin liner capacity for crude oil retention over time.

One way to determine how much crude oil a sorbent material can hold is to do an oil retention capacity test in a lab. The ratio of oil adsorbed to the weight of dry sorbent was used to calculate oil retention [23]:

$$\text{Crude oil capacity } \% = (Os - On)/Os \qquad \text{--------} \ (1)$$

Where: Os is the total crude oil sorption, and On is the net crude oil remaining.

The test procedure includes the preparation of 10 liners depending on kaolin grain size ranging from 300, 150, 75, 50 µm and nano size with chosen crude oil (light and heavy).

3. Results

3.1 Kaolin characterization

XRD pattern of kaolin from the western desert in Iraq is shown in Figure 1. As reported by Worasith et al, (2011), the majority of the peaks can be accounted for by the kaolin minerals; the strong peaks at 2θ =11.9˚, 19.6˚ and 24.6˚ with d spacing 7.41, 4.52 and 3.61 A˚ correspond to the kaolinite d001, d002 and d060 reflections [24]. In addition, peaks at 2θ = 35.6˚, 39.1˚, 59.7˚ and 62.1˚ with d spacing 2.51, 2.3, 1.5 and 1.45A˚ are all consistent with kaolinite. Illite, which is a common impurity in kaolin minerals, is seen by the presence of major peaks at 4.52, 2.51 and 2.3 A˚ in addition to those mentioned above. In addition, weak peaks at 3.07 A˚ could correspond to the main reflections from montmorillonite. The presence of quartz is seen by its principal reflection at 3.37 A˚, and minor peak at 1.82 A˚. The XRD pattern of nano kaolin is shown in Figure 2. Grinding of the clay to nano size gives no significant shift of kaolinite peaks and remained sharp; the strong reflection at 2θ =11.9˚ and 24.6˚ shift to 11.01˚ and 24.9˚. Reducing kaolin grain size resulted in a major decrease in the relative intensities of the peaks from the kaolinite and illite phases (Figure 2), consistent with appreciable structural damage to these minerals.

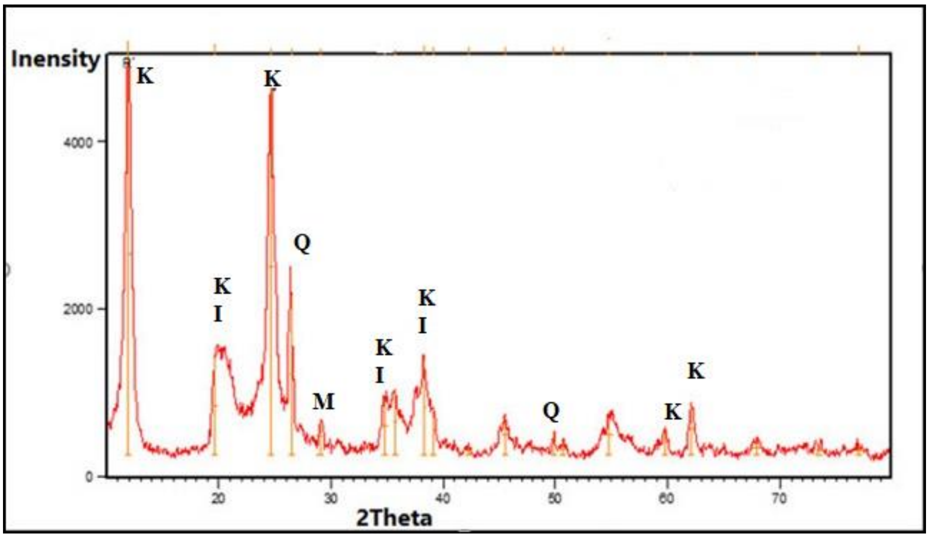

Figure 1: X-ray analysis of kaolin.

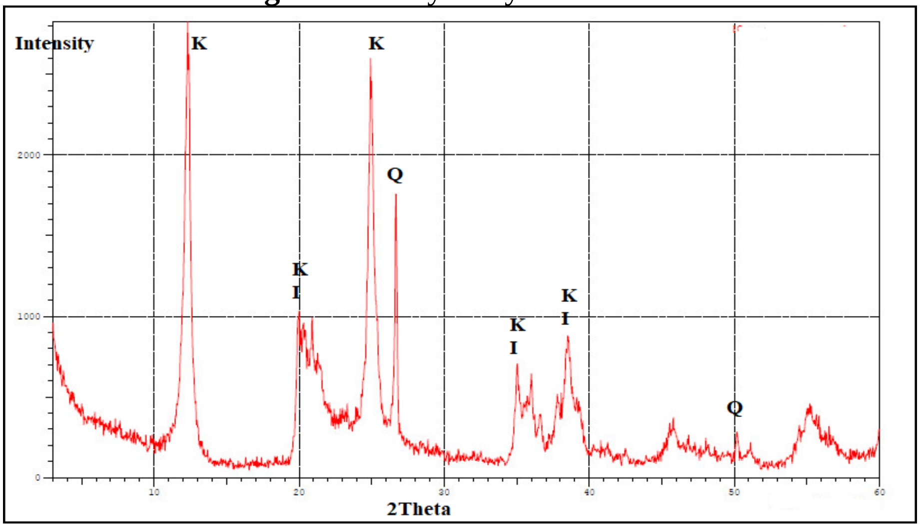

Figure 2: X-ray analysis of nano grain size kaolin.

Table 2 illustrates the chemical composition of Iraqi kaolin. SiO_2 and Al_2O_3 are the dominant components, followed by Fe_2O_3. Due to the lack of carbonates, there is a low concentration of CaO and MgO. In western desert kaolin, SiO_2 content is 46.48 wt. %, Al_2O_3 is 35.45 %. There are also minor amounts of Fe_2O_3 1.62 % and TiO_2 1.6 % and smaller concentrations of Na_2O, CaO, MgO, MnO, SO_3 and K_2O. The chemical composition of Iraqi kaolin is similar to that of pure kaolin in that it contains SiO_2 and Al_2O_3 in amounts of 46% and 40%, respectively [1].

Table 2: Kaolin chemical composition.

SiO_2 %	Al_2O_3%	Fe_2O_3%	CaO%	MnO%	MgO%	Na_2O%	SO_3%	K_2O%	TiO_2%
46.48	35.45	1.62	0.56	0.19	0.14	0.16	0.19	0.48	1.6

3.2 FTIR Spectroscopy

The FTIR spectrum of the Iraqi kaolin (Figure 3A) shows the typical kaolinite bands, which correspond to structural bonds: tetrahedral silica (Si–O), octahedral aluminium (Al–O and Al–OH) and SiO_4–Al_2O_3 bonds (Si–O–Al). Iraqi kaolin absorbance bands positions and assignments have been compared to those of theoretical kaolinite [25]. The most distinctive kaolinite absorption bands, which conform to structural water and Al-OH stretching vibrations, are observed in the range between 3800 and 3600 cm^{-1} [25] [26] [27]. In Iraqi kaolin, these FTIR bands appear at 3693.8**,** 3656.8 and 3621.1 cm^{-1}. The band at 3693.4 cm^{-1} arises from surface hydroxyls and produces an in-phase vibration perpendicular to the 1:1 layers [28]. Stretching vibrations that are sub-parallel to the 1:1 layers produced the band 3656.8 cm^{-1}. The fourth inner OH group is represented by the lowest frequency band at 3621.1 cm^{-1}. The band at 3621 cm^{-1} is hydroxyl groups on the octahedral alumina layer surface that are linked to oxygen atoms from the adjacent silica tetrahedral layer [29]. The bands between 3694 and 3619 cm^{-1}, which appear at 3693.8**,** 3656.8 and 3621.1 cm^{-1} in this sample, reveal a well-ordered kaolinite structure [25]. Moreover, the band 1642.3 cm^{-1} is corresponding to H-O-H stretching. The bands at 1116.7,1030.09, and 1003.6 cm^{-1} occur in the region corresponding to Si-O stretching, located between 945 and 1120 cm^{-1}. Si-O, Al-O stretching modes, and OH deformation are assigned to the 912.6 cm^{-1} band. Also, bands at 750.1 and 687.8 cm^{-1} are corresponding to Si-O [27].

Figure 3B shows the FTIR, including the nano kaolin after crude oil saturation. The FTIR displays additional bands associated with the organic components. The band 1451.7 cm^{-1} was assigned to aromatic C-H stretching vibration [30]. The absorption bands at 2924.2 and 2853.6 cm^{-1} were related to asymmetric and symmetric aliphatic CH_2 groups, respectively [27]. The absorption spectra of saturated kaolin appeared to be new bands from those of unsaturated clay, suggesting that organic components adsorb on the clay surface.

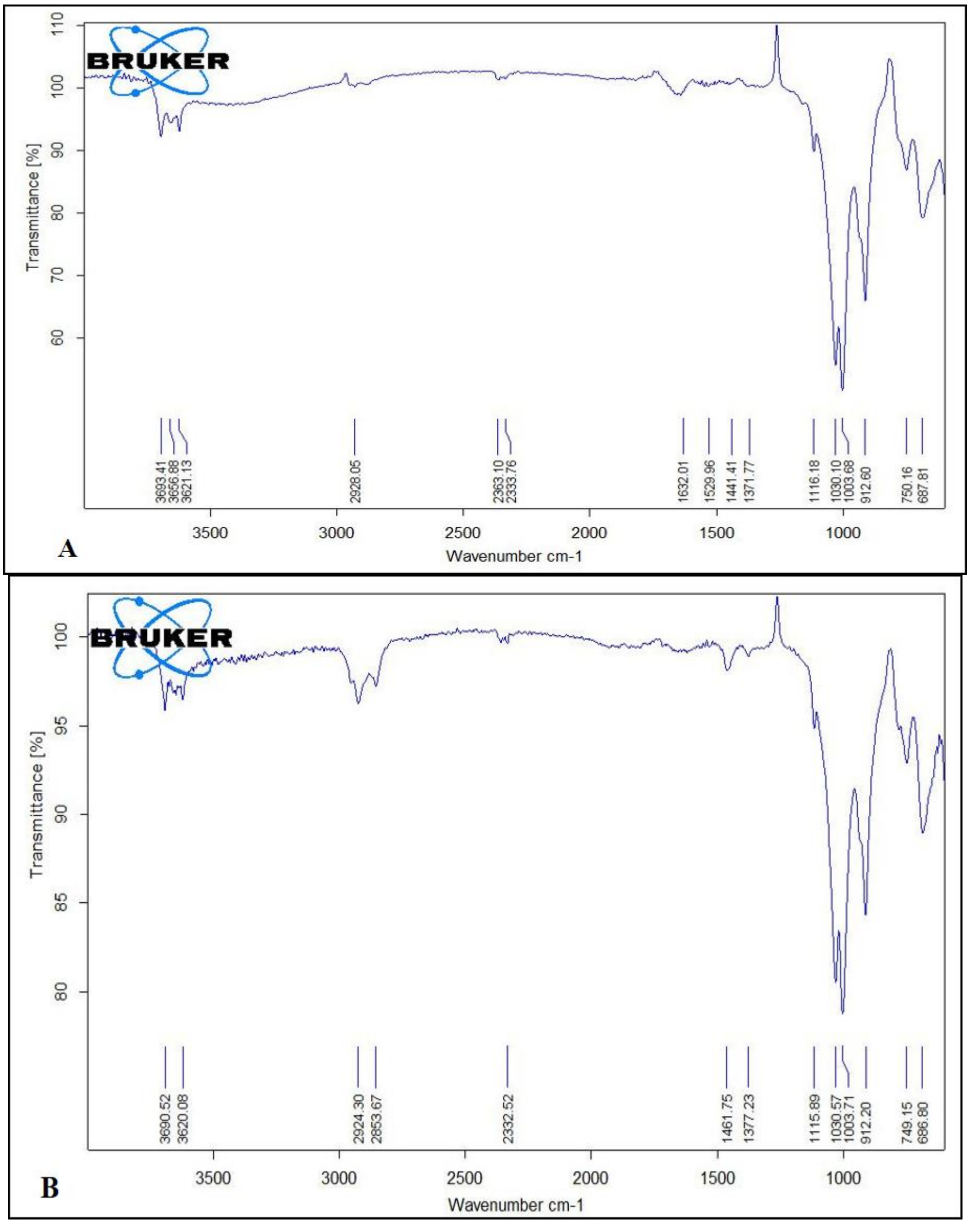

Figure 3: (A) shows the FTIR of the Iraqi kaolin before saturation. (B) shows the FTIR including the nano kaolin after crude oil saturation.

3.3 Particle size

Kaolin particle size distribution has a significant influence on controlling viscosity, and shrinkage properties [25]. The particle size distribution of kaolin determines its suitability for various applications. This study investigated kaolin particles with a nano size, equal to or less than 300 μm. Figure 4 shows the particle size distribution results. According to the figure, the particle size distribution of nano kaolin ranges from minimum size 38.1nm to maximum size 48.1nm, with the particle size median at 42.8 nm, mean at 42.9 nm, and skewness at 0.154.

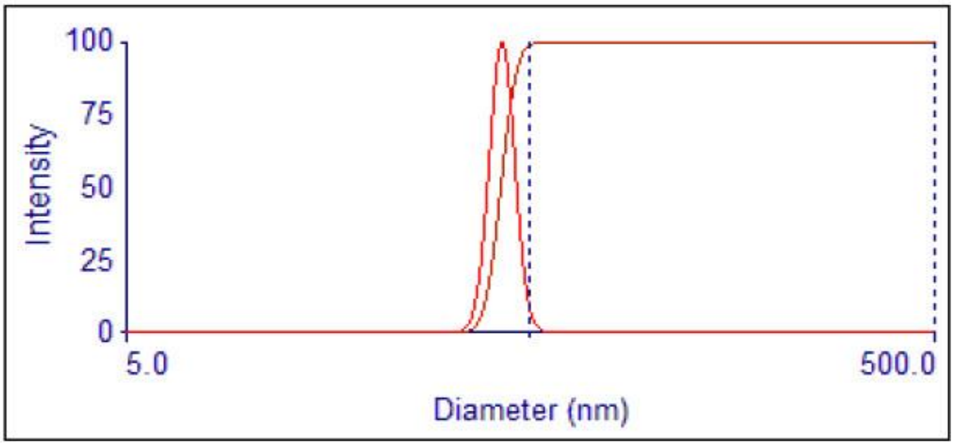

Figure 4: Lognormal size distribution of kaolin (nm).

3.4 kaolin liner with heavy crude oil

Four kaolin liners of varying grain sizes were tested to determine the effect of grain size on their capacity to hold heavy crude oil. The kaolin liner saturation rate with various grain sizes over time is shown in Table 3 and Figure 5. Both liner 50 µm and liner 300 µm failed to restrict and contain crude oil, and as a result, oil spilt after 54 and 72 hrs, respectively. Liners 75 µm and 150 µm were able to restrict and contain crude oil for a more extended period of time than liners 50 µm and 300 µm, as the oil leaked after 90 and 96 hrs, respectively.

In general, kaolin 300, 150, 75 and 50 µm failed to impede and prevent the movement of pollutants. Thus, kaolin is totally inefficient. Furthermore, grinding kaolin to 50 µm and 75 µm reduced its efficiency in terms of crude oil retention compared to grain sizes 150 µm and 300 µm.

Table 3: Saturation rate of kaolin with heavy crude oil (Al-Ahdab crude oil).

300 µm		**150 µm**		**75 µm**		**50 µm**	
saturation rate %	**Time (hr)**	**saturation rate %**	**Time (hr)**	**saturation rate %**	**Time (hr)**	**saturation rate %**	**Time (hr)**
0	0	0	0	0	0	0	0
4.4	1	5.5	1	6.67	1	8.9	1
8.9	2	10	2	11.1	2	17.8	2
11.1	3	12.3	3	13.3	3	20	3
15.6	5	16	5	17.7	5	24.5	5
20	10	21.5	10	23.9	10	31.1	10
24.4	15	27	15	30	15	40	15
28.9	20	32.5	20	36.1	20	45.7	20
33.3	25	37.3	25	42.2	25	50	25
46.7	30	50.7	30	54.4	30	62.2	30
51.1	35	54.1	35	57.8	35	68.9	35
53.3	40	59.2	40	61.5	40	74.7	40
56.4	45	63	45	66.7	45	82.2	45
60	50	67.7	50	71.7	50	89	50
75.6	55	72	55	76.8	55	100	54
81.7	60	77.5	60	80	60	-	-
88.9	65	84	65	83.9	65	-	-
97.8	70	94	70	88.9	70	-	-
100	72	96	75	92.4	75	-	-
-	-	97.8	80	95.5	80	-	-
-	-	99	85	97.6	85	-	-
-	-	100	90	98.7	90	-	-
-	-	-	-	100	96	-	-

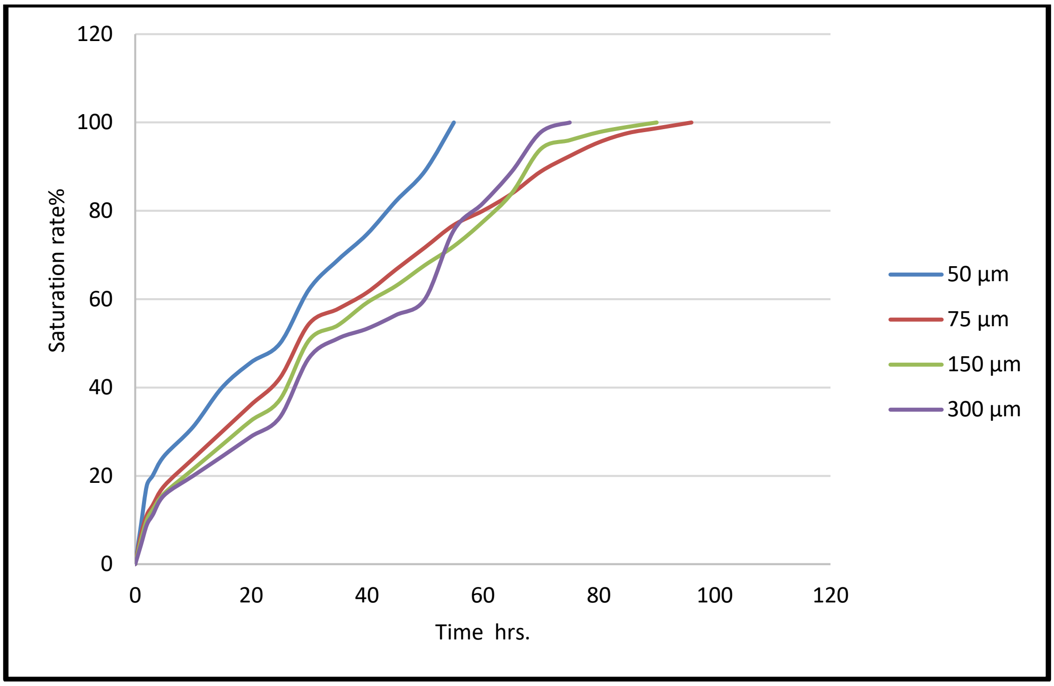

Figure 5: Saturation rate kaolin with heavy crude oil (Al-Ahdab crude oil).

3.5 kaolin liner with light crude oil

These tests assess the ability of kaolin 50, 75, 150 and 300 µm as a liner in preventing light crude oil spills. Kaolin sorption capacity (AC%) (50, 75, 150, and 300) µm equals zero. Soon after adding crude oil to kaolin, cracks form that cause crude oil to spill completely, resulting in no sorption. All experiments failed, even when repeated more than once for Al-Burjsiha crude oil.

3.6 Nano-sized kaolin liner

Two liners were formed by substituting 25% of kaolin 150 µm with nano kaolin (nanosized kaolin liner), then tested with chosen crude oil. Table 4 depicts the behaviour of heavy crude oil with a nano kaolin liner. After 410 hrs, nano kaolin liner reaches a maximum saturation rate of 41.4%, while 150 µm kaolin liner reaches 100% saturation and seepage after 90 hrs. Compared to a liner made entirely of kaolin 150 µm, adding 25% nano clay makes the liner more cohesive, allowing it to stop heavy crude oil seepage. The saturation rate of liners with light crude oil is depicted in Table 4. The nano kaolin liner keeps roughly 36% of its oil after 310 hrs, whereas kaolin liner 150 µm loses oil almost immediately after being put over clay. Adding nano size to a liner reduces light crude oil diffusion through the liner and increases cohesion, which could prevent light crude oil seepage.

Table 4: shows the saturation rate of nano kaolin with heavy (Al- Ahdab) and light crude oil (Al–Burjsiha).

Al–Burjsiha crude oil		**Al–Burjsiha crude oil**		**Al-Ahdab crude oil**		**Al-Ahdab crude oil**	
Kaolin 150 µm		**Kaolin 150 µm + Nano kaolin**		**Kaolin 150 µm**		**Kaolin 150 µm + Nano kaolin**	
saturation rate %	**Time (hr)**	**saturation rate %**	**Time (hr)**	**saturation rate %**	**Time (hr)**	**saturation rate %**	**Time (hr)**
0	0	0	0	0	0	0	0
0	0	0.4	1	5.5	1	11	1
0	0	1.2	2	10	2	15	2
0	0	1.2	3	12.3	3	20	3
-	-	1.9	5	16	5	24	5
-	-	2.2	10	21.5	10	27	10
-	-	9.1	20	27	15	28.5	20
-	-	14.6	30	32.5	20	31	30
-	-	16.1	40	37.3	25		↓
-	-	17	50	50.7	30	31	170
-	-	19	60	54.1	35	32.2	180
-	-	21	70	59.2	40	34.5	190
-	-	22.3	80	63	45	34.5	200
-	-	24.4	90	67.7	50	34.5	210
-	-	25.1	100	72	55	35.2	230
-	-	25.7	120	77.5	60	35.8	250
-	-	26.1	140	84	65	36.8	270
-	-	27.7	160	94	70	37.4	290
-	-	29.2	180	96	75	38	310
-	-	30	200	97.8	80	38.9	330
-	-	31.6	240	99	85	39.3	350
-	-	32.4	280	100	90	40.3	370
-	-	33.6	320	-	-	41.4	390
-	-	35.6	360	-	-	41.4	410
-	-	37.4	400	-	-	41.4	450
-	-	37.7	440	-	-	41.4	500
-	-	37.7	480	-	-	41.4	550
-	-	37.7	520	-	-	-	-
-	-	37.7	560	-	-	-	-

4. Discussion

4.1 Effect of kaolin particle size

Kaolinite has a relatively simple structure and crystallizes as a periodic arrangement of T-O layers stacked along the c-axis, forming fundamental particles of a specific crystallite size (nm). These nano-sized particles are typically agglomerated, resulting in platy pseudohexagonal micromorphology aggregates [6]. Kaolin aggregates are booklets forming vermiform aggregates common in most kaolin [31]. The physical properties of clays are influenced by the shape and size of clay particles, as well as aggregate characteristics. Therefore, grinding kaolin to a nanoscale may be a good technique for increasing kaolin liner efficacy. The results clearly demonstrated the importance of particle size as a controlling factor of kaolin liner properties. Within the first five hours, the saturation rate of kaolin liners (50, 75, 150, and 300 µm) increased significantly. After that, the rate of liner saturation increased gradually over an extended period of time, reaching 100% saturation after 54, 96, 90, and 72 hrs for lines of 50, 75, 150, and 300 µm, respectively.

This is consistent with the findings of other researchers [17] and [13], who found that the rate of clay liner saturation increased significantly within the first five hours and then gradually over a significant amount of time. The impact of particle size can be plainly seen when comparing a liner composed entirely of kaolin 150 µm to one made of 25% nano kaolin and 75% kaolin 150 µm. Within the first five hours, the saturation rates for both kaolin liners (nano and 150 µm) rose sharply by 24% and 16%, respectively, for heavy crude oil. It has been demonstrated that kaolin particles aggregate with oil to form OMAs (oil-mineral aggregations). Kaolin particles tend to attach to the surface of oil droplets and become dominant in small-sized flocs in the mixture sample [22] [23]. Because highly active sites are available at the beginning of the process, according to Al-Bidry and Hamed (2022) [13], attachment happens quickly, especially with nano linesr. After that, as time passed and equilibrium was reached, the saturation rate gradually increased until it reached 41.4% for nano liner after 410 hrs without a spill. Liner 150 µm reached 100% saturation after 90 hrs, at which point spillage started. This might make up most of the nano clay in tiny flocs with oil in the liner mixture and clog the pore and preventing seepage.

4.2 Effect of crude oil viscosity

The effectiveness of kaolin is impacted by several factors, including the viscosity of crude oil. The findings of this study demonstrated that crude oil viscosity had a significant impact on kaolin's effectiveness. Kaolin liners (50, 75, 150 and 300 µm) failed to stop light crude oil seepage. The influence of crude oil viscosity on the efficacy of the kaolin liner is easily visible when comparing a liner of 150 µm to nano kaolin with different crude viscosity oil. Notice, liner 150 immediately leaks light crude oil when added with a saturation rate of 0%. With a saturation rate of 37.4% after 400 hrs, the nano kaolin liner, on the other hand, kept light crude oil and prevented oil from spilling out. The number of droplet OMAs is strongly correlated with the viscosity ratio, and droplet concentration decreases rapidly as oil viscosity increases. It has been proposed that changes in volume concentration with viscosity are related to changes in the number of oil droplets rather than their sizes. Droplet concentration decreases rapidly as oil viscosity increases, and the number of droplet OMAs is strongly correlated with the viscosity ratio. Volume concentration changes with viscosity are related to changes in the number of oil droplets rather than their sizes [23] [32]. Reducing grain to nano size increases kaolin particles, that aggregate with oil, and form OMAs. Increasing OMAs concentration can cause the screening of surface negative charges and block pores by oil leading to a decrease in the saturation rate of crude oil. It is possible to infer from this that as OMAs increased, the ability for sorption within pores became less active and crude oil diffusion within the liner decreased. As a result, the saturation rate declined to 1.9% and 37.4% after 5 and 400 hours, respectively.

5. Conclusion

Using local kaolin with nano-sized particles in the liner makes the liner more effective at stopping the leakage of crude oil. Several conclusions could be drawn from this research, including the ones below:

- Kaolin liners (50, 75, 150, and 300 µm) failed to stop seepage and retention of crude oil, so they could not be used as the main liner to stop light crude oil flow.
- For heavy crude oil, kaolin liners 50 µm and 300 µm had retention and seepage prevention for 54 and 72 hrs, respectively. While liners 75 µm and 150 µm were able to retain and prevent seepage of heavy crude oil for 96 and 90 hrs, respectively
-Partial replacement of kaolin 150 µm by nano-size kaolin improved the ability of the liner to impede the flow of light and heavy oil with a long period of retention time and without seepage.
-Low-viscosity crude oil frequently seeps through compacted clay liners, which is common. With the addition of nano-sized kaolin, a liner that may be used to prevent crude oil spills of any viscosity was created. It is an efficient engineered barrier system for crude oil of any viscosity, and that can be used as a compacted liner.

References

[1] R Dewi, H Agusnar, Z Alfian and Tamrin, "Characterization of technical kaolin using XRF, SEM, XRD, FTIR and its potentials as industrial raw materials", *IOP Conf. Series: Journal of Physics: Conf. Series 1116 - 042010*, 2018, Doi:10.1088/1742-6596/1116/4/042010.

[2] JP Temga, JP Macheb, AB Madib, JP Nguetnkamc and DL Bitomd, "Ceramics applications of clay in Lake Chad Basin, Central Africa", *Applied Clay Science*, vol. 171, pp. 181-132, 2019, https://doi.org/10.1016/j.clay.2019.02.003.

[3] JP Temga, A Balo Madi, S Basga Djakba, P Zo'o Zame, M Abessolo Angue, JR Mache, JP Nguetnkam and LD Bitom, "Lime – and sand – stabilization of clayey materials from the Logone valley (Lake Chad basin) for their utilization as building materials", *J. Build. Eng.*, vol. 19, pp. 472–479, 2018, https://doi.org/10.1016/j.jobe.2018.06.003.

[4] F Pardo, MM Jordan and MA Montero, "Ceramic behaviour of clays in Central Chile", *Appl. Clay Sci.*, vol. 157, pp.158–164, 2018, https://doi.org/10.1016/j.clay.2018.02.044.

[5] ME Awad, A Borrego-Sánchez, E Escamilla-Roa, A Hernández-Laguna and I Sainz-Díaz, "Modelling of the adsorption of a protein-fragment on kaolinite with potential antiviral activity", *Applied Clay Science*, vol. 199, pp.105865, 2020, https://doi.org/10.1016/j.clay.2020.105865.

[6] ME Awad, LG Alberto, SE Rita, ISD Claro, MR Mahmoud and V César, "Crystallite size as a function of kaolinite structural order-disorder and kaolin chemical variability: Sedimentological implication", *Applied Clay Science*, vol. 162, pp. 261–267, 2018, https://doi.org/10.1016/j.clay.2018.06.027.

[7] MA Al-Birdy, "Chemistry and Mineralogy of Iraqi Kaolin and Application as a Filter", *AIP Conference Proceedings 2443, 030037*, 2022, https://doi.org/10.1063/5.0091858.

[8] Z Halyna , K Vadym , S Stella and R Serhii, "Particle size distribution and crystallinity as indicators of kaolinite genesis", *Applied Clay Science*, vol. 213, no. 1, pp. 106236, 2021, https://doi.org/10.1016/j.clay.2021.106236.

[9] B Akbari, TM Pirhadi and M Zandrahimi, "Particle size characterization of nanoparticles–A practical approach", Iranian *Journal of Materials Science & Engineering*, vol. 8, no. 2, 2011.

[10] JP Amber, B Bhuvnesh and GB Michael, "Nano-enhanced Bioremediation for Oil Spills: A Review", *ACS EST Engg.*, vol. 1, no. 6, pp. 928–946, 2021, https://doi.org/10.1021/acsestengg.0c00217.

[11] K Qiao, W Tian, J Bai, L Wang, J Zhao, Z Du and X Gong, "Application of magnetic adsorbents based on iron oxide nanoparticles for oil spill remediation: A review", J. *Taiwan Inst. Chem. Eng.*, vol. 97, pp. 227– 236, 2019.

[12] RK Rowe, "Geosynthetic clay liners: Perceptions and misconceptions", *Geotextiles and Geomembranes*, vol. 48, no, 2, pp. 137-156, 2020, https://doi.org/10.1016/j.geotexmem.2019.11.012.

[13] MA Al-Bidry and RS Hamied, "Utilizing attapulgite as anti-spill liners of crude oil", *Baghdad Science Journal*, vol, 19, no. 3, pp. 693-703,2022, https://doi.org/10.21123/bsj.2022.19.3.0690.

[14] S Gitipour, MA Hosseinpour, N Heidarzadeh, P Yousefi and A Fathollahi, "Application of modified clays in geosynthetic clay liners for containment of petroleum contaminated sites", *Int. J. Environ. Res*, vol. 9, no. 1, pp. 317-322, 2015.

[15] SA Naeini, N Gholampoor and MA Jahanfar, "Effect of leachate's components on undrained shear strength of clay-bentonite liners", *Euro. J. Envi. Civil Eng.*, vol.15, pp, 1-14, 2017, https://doi.org/10.1080/19648189.2017.1278725.

[16] S Javadi, M Ghavami, Q Zhao, and B Bate, "Advection and retardation of non-polar contaminants in compacted clay barrier material with organo clay amendment", Appl. *Clay Sci*., vol. 142, pp. 30-39, 2017, https://doi.org/10.1016/j.clay.2016.10.041.

[17] MA Al-Bidry, RS Hamied and G Raja, "Anti-spill of compacted Iraqi bentonite by using different Iraqi crude oil", *Emirates Journal for Engineering Research*, vol. 22, no. 2, pp. 11-16, 2017.

[18] V Zotiadis and A Argyraki, "Development of innovative environmental applications of attapulgite clay", *Bulletin Geo. Soc. Greece*, vol. 47, no, 2, pp. 992-1001, 2017, doi.org/10.12681/bgsg.11139.

[19] JK Mitchell and K Soga, "Fundamentals of soil behavior", 3rd Edition, *John Wiley and Sons Inc., New York, USA*, ISBN: 978-0-471-46302-3, pp. 592, 2005.

[20] RB Oyeleke, M Badruddin, M Razman and A Kamaruddin, "Compaction parameters of kaolin clay modified with palm oil fuel ash as landfill liner", IEEE *First Conference on Clean Energy and Technology CET*, 2011, DOI: 10.1109/CET.2011.6041463.

[21] G Yucel, C Bora, AH Aydilek, BF Tanyu and K Savas, "Utilization of sepiolite materials as a bottom liner material in solid waste landfills", *Waste Management*, vol. 34, pp, 112-124, 2014.

[22] L Ye, AJ Manning, J Holyoke, A Jorge, Penaloza-Giraldo and TJ Hsu, "The Role of biophysical stickiness on oil-mineral flocculation and settling in seawater", *Frontiers in Marine Science*, vol. 8, 2021, https://doi.org/10.3389/fmars.2021.628827.

[23] A Khelifa, P Stoffyn-Egli, PS Hill and K Lee, "Characteristics of oil droplets stabilized by mineral particles: effects of oil type and temperature", *Spill Sci. Technol. Bull*, vol. 8, pp.19–30, 2002, Doi: 10.1016/s1353-2561(02)00117-2.

[24] N Worasith, BA Goodman, J Neampan, N Jeyachoke and P Thiravetyan, "Characterization of modified kaolin from the Ranong deposit Thailand by XRD, XRF, SEM, FTIR and EPR techniques", *Clay Minerals*, vol.46, pp. 539–559, 2011, DOI: 10.1180/claymin.2011.046.3.539.

[25] CV Maite, A Pura, M Salvador and R Núria, "Mineralogical and thermal characterization of kaolinitic clays from Terra Alta (Catalonia, Spain)", *Minerals*, vol. 10, no. 142, 2020, http://dx.doi.org/10.3390/min10020142.

[26] C Shichao, H Anmin, W Shennan and Z Qiuhui, "Effect of deferent heat treatment temperatures on the chemical composition and structure of Chinese Fir wood", *Bio Resources*, vol.11, no.2, pp. 4006–4016, 2016, http://dx.doi.org/10.15376/biores.11.2.4006-4016.

[27] Y Yanshan, Y Huixia, W Zihua, Q Caiwen, T Hong, Z Wei, H Zhangmao and F Leihua, "Characterization of coals and coal ashes with high Si content using combined second-derivative Infrared spectroscopy and Raman Spectroscopy", Crystals, vol. 9, no.10, pp. 513, 2019, http://dx.doi.org/10.3390/cryst9100513.

[28] L Vaculíková, P Eva, V Silvie and K Ivan, 'Characterization and differentiation of kaolinites from selected Czech deposits using infrared spectroscopy and deferential thermal analysis", *Acta Geodynamica et Geomaterialia*, vol. 8, no. 1, pp. 59–67, 2011.

[29] R Dewi , H Agusnar, Z Alfian and Tamrin, 'Physiochemical characterization of natural kaolin from Jaboi Indonesia', *Rasayan J. Chem.*, vol. 13, no. 1, pp. 382-388. 2020, http://dx.doi.org/10.31788/RJC.2020.1315523.

[30] HP Signe, S Lee, F Xavier and K Dmitry, "Complementarity of Raman and Infrared spectroscopy for rapid characterization of fucoidan extracts", *Plant Methods*, vol. 17, no. 130, 2021, https://doi.org/10.1186/s13007-021-00830-6.

[31] GE Christidis, "Industrial clays", *EMU Notes in Mineralogy*, vol. 9 , Chapter 9, pp. 341–414, 2011.

[32] C Onuma, F Ray, X Yunfei and K Serge, "Adsorption of hydrocarbons on organo-clays-implications for oil spill remediation", Journal *Colloid and Interface Science,* vol. 305, no. 1, pp. 17-24, 2007.